Journal of Solid State Chemistry **163,** 93–99 (2002)
doi:10.1006/jssc.2001.9377, available online at http://www.idealibrary.com on IDEAL®

High Lithium Capacity $M_xV_2O_5A_y \cdot nH_2O$ for Rechargeable Batteries

C. C. Torardi,[1] C. R. Miao, M. E. Lewittes, and Z. Li

DuPont Company, Central Research and Development, Experimental Station, Wilmington, Delaware 19880-0356

Received February 26, 2001; in revised form August 21, 2001; accepted August 24, 2001

The aqueous synthesis and electrochemical properties of nanocrystalline $M_xV_2O_5A_y \cdot nH_2O$ are described. It is easily and quickly prepared by precipitation from acidified vanadate solutions. $M_xV_2O_5A_y \cdot nH_2O$ has been characterized by X-ray powder diffraction, electron microscopy, TGA, chemical analyses, and electrochemical studies. The atomic structure is related to that of xerogel-derived $V_2O_5 \cdot nH_2O$. In $M_xV_2O_5A_y \cdot nH_2O$, M is a cation from the starting vanadate salt and A is an anion from the mineral acid. This material exhibits high, reversible Li capacity and may be considered for use in a cathode in primary and secondary batteries. The lithium capacity of an electrode composed of $M_xV_2O_5A_y \cdot nH_2O$/EPDM/carbon (88/4/8) is ~ 380 (mA h)/g (C/80 rate) and the energy density is ~ 1000 (W h)/kg (120-μm-thick cathode, 4–1.5 V, versus Li metal anode). Critical parameters identified in the synthesis of $M_xV_2O_5A_y \cdot nH_2O$, with respect to achieving high Li-ion insertion capacity, are acid/vanadium ratio, starting vanadate salt, and temperature. Inclusion of carbon black in the synthesis yields a composite that maintains the high Li capacity, lowers the electrochemical-cell polarization, and preserves the lithium capacity at higher discharge rates. Li-ion coin cells, using prelithiated graphite anodes, exhibit electrochemical performance comparable to that of Li-metal coin cells. © 2002 Elsevier Science

Key Words: **vanadium oxide hydrate; vanadate hydrate; lithium vanadate; lithium battery; rechargeable battery.**

INTRODUCTION

Vanadium-oxide-based materials have been studied extensively for use in cathodes for rechargeable lithium batteries. Many vanadium-oxide compounds are easy to synthesize, have acceptable production costs, and have good lithium capacity. The primary disadvantage is their poor cycle life. Nevertheless, vanadium oxides still attract attention, and research continues with the goal of improving electrochemical behavior.

One area of study involves the layered vanadium-oxide hydrates. These oxide hydrates, usually described by the formula $V_2O_5 \cdot nH_2O$, can be synthesized by various methods. Livage has described vanadium oxide sol–gel chemistry as one technique to make the layered hydrates (1). Much work on xerogel and aerogel synthesis of $V_2O_5 \cdot nH_2O$ for battery applications has been done in the laboratories of W. H. Smyrl at the University of Minnesota (2). Some of these sol–gel-derived compositions have been shown to have very high lithium capacities. As a recent example, M. Giorgetti *et al.* (3) discuss a fibrous $V_2O_5 \cdot nH_2O$ xerogel product with sufficiently high lithium insertion capacity to make it attractive as an electrode-active material in lithium batteries (~ 340 (mA h)/g at a C/55 rate).

Another method to make vanadium-oxide hydrates, having nominal composition $V_2O_5 \cdot nH_2O$, involves precipitation from aqueous vanadate solutions by addition of mineral acid (4). However, the resulting products have been described as being of low yield, highly contaminated, and of variable properties (5, 6). We report here a facile acid-precipitation method that makes a nonfibrous $V_2O_5 \cdot nH_2O$-related product in high yield and that gives highly reproducible chemical compositions and lithium capacities. In comparison to the xerogel method, acid precipitation is a much simpler and cheaper synthesis procedure and yields a material having equivalent or higher lithium capacity.

EXPERIMENTAL

Synthesis

The general synthesis process for $M_xV_2O_5A_y \cdot nH_2O$ consists of preparing an aqueous vanadate salt solution, heating at or close to the boiling temperature, and precipitating the product with a strong mineral acid. The vanadium concentration is typically in the range of 0.1–1 M. Suitable vanadate salts include NH_4VO_3, $LiVO_3$, $NaVO_3$, KVO_3, $RbVO_3$, and MgV_2O_6. However, the salts that give products having the highest lithium capacities are NH_4VO_3, $LiVO_3$, and MgV_2O_6. As an alternative, V_2O_5 can be combined with an aqueous ammonium, alkali, or alkaline earth hydroxide to form a corresponding vanadate solution. A strong mineral acid is added to the hot solution to provide an acid proton to vanadium ratio (designated the

[1] To whom correspondence should be addressed. Fax: (302)695-1664. E-mail: charlie.c.torardi@usa.dupont.com.

0022-4596/02 $35.00

"H/V ratio") in the range of about 0.70:1 to 6:1. Suitable acids for the synthesis are H_2SO_4, HNO_3, and HCl. In the case of vanadate salts of NH_4, Na, K, and Rb, the acid to vanadium ratio must be high enough, typically at least 1:1, to avoid or minimize the co-formation of $M_2V_6O_{16}$. Following isolation, drying, grinding, and sieving (− 200 mesh), the nominally $V_2O_5 \cdot nH_2O$ powder is ready for incorporation into an electrode.

Synthesis Example

NH_4VO_3 (20.1 g) was dissolved in 900 mL of deionized water while stirring with a Teflon-coated magnetic stirring bar in a 1-L Pyrex beaker. The contents of the beaker were heated to the boiling point to form a solution. Concentrated H_2SO_4 (9.6 mL) diluted in 25 mL of deionized H_2O was added. The duration of heating after acid addition was 20 min. The H/V ratio was 2.

The beaker was then removed from the heat and stirring discontinued. The reddish-brown solids were allowed to settle for 5 min. About 600 mL of supernatant liquid was decanted, and 700 mL of fresh H_2O was added to the precipitate in the beaker and then reslurried by stirring for about 1 min. The solids were allowed to settle, and the cycle of decanting, fresh water addition, and reslurrying was repeated. After settling and decanting the second wash liquid, the product was collected on filter paper by suction filtration. The moist cake was easily crumbled onto a large cover glass and dried under an infrared heat lamp for several hours to give 16.2 g of product. A composition of $(NH_4)_{0.12}V_2O_5(SO_4)_{0.06} \cdot 0.8H_2O$ was derived from chemical and thermogravimetric analyses. On the basis of this composition, a product yield of 92% was calculated. The brick-red product was shown to be nonfibrous by SEM images, which is different from the fibrous morphology reported for xerogel and aerogel syntheses. An X-ray powder diffraction pattern showed only the broad lines characteristic of the nominal $V_2O_5 \cdot nH_2O$ composition prepared by our acid-precipitation method (Fig. 1). The sieved product (− 200 mesh) was cast into an electrode, assembled into coin cells, and tested as described below. The discharge capacity was determined to be 370 (mA h)/g (at a discharge rate of ~ C/80).

X-Ray Powder Diffraction

Room-temperature X-ray powder diffraction data were obtained using an APD3720 powder diffractometer with a theta compensating slit, graphite monochromator, and Cu radiation.

Electron Microscopy

Scanning and transmission electron microscopy was used to characterize the microstructure of $M_xV_2O_5A_y \cdot nH_2O$.

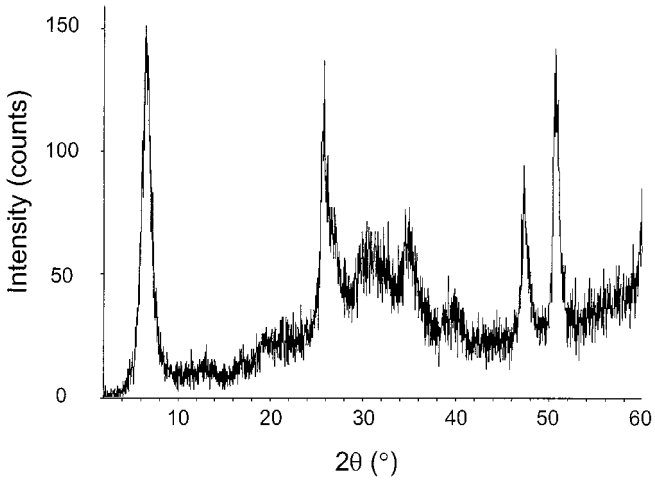

FIG. 1. Typical X-ray powder diffraction pattern for $M_xV_2O_5A_y \cdot nH_2O$.

This work was done with a JEM-2000EX transmission electron microscope having an interpretable resolution of better than 0.27 nm.

Electrochemical Measurements

To make an electrode, 1.5000 g of −200-mesh sieved powder was combined with 0.1364 g of Super P carbon black (MMM S.A. Carbon, Brussels, Belgium) and 1.705 g of a 4 wt% solution of Nordel EPDM (DuPont, ethylene propylene diene monomer) rubber in cyclohexane. An additional 2.5 mL of cyclohexane was added to improve flow. The mixture was shaken in a capped glass vial for 15 min on a mechanical shaker to form a cathode paste.

The cathode paste was spread onto a sheet of Teflon FEP (DuPont) and drawn down to form a film using a doctor blade having a 15-mil gap. The dried film, consisting of 88% by weight active powder, 4% by weight binder, and 8% by weight carbon black, was hot-pressed through a calender roller between Kapton polyimide sheets (DuPont) under 20 psi at 110°C. The thickness of the films was typically 80–150 μm.

The consolidated electrode films were examined as cathodes against Li metal anodes in coin cells. $LiPF_6$ in EC/DMC (ethylene carbonate/dimethyl carbonate from E.M. Industries) served as the electrolyte solution. A glass fiber separator was used between the electrodes. Disks of cathode (1.40 cm^2), anode (~ 1.33 cm^2), and separator (2.54 cm^2) were cut with punches. In a dry helium atmosphere, electrolyte solution was added to the cathode and separator pieces that were stacked along with the Li and a spacer into a coin-cell pan and sealed under pressure using the 2325 Coin Cell Crimper System manufactured by the National Research Council of Canada.

Electrochemical measurements were performed with a Maccor series 4000 tester (Maccor, Inc., Tulsa, OK) and Version 3.0 (SP1) software. The coin cells were tested over the range of 4–1.5 V. The measurement of discharge capacity began with a constant current of 0.5 mA. When the voltage reached 1.5 V, the discharge mode was changed to constant voltage and the current allowed to slowly decay to one-tenth the original value, i.e., 0.05 mA. This constant voltage portion of the discharge, which allows the cell to nearly reach equilibrium, has the effect of reducing the potential drop from the current so that the remaining cell polarization is principally due to the over potential required for lithium insertion into the cathode material. The discharge capacity is the integrated charge transfer during both the constant current and constant voltage portion of the discharge.

After discharge, the cell was charged by reversing the above process, using a constant current of 0.5 mA until a maximum voltage of 4.0 V was reached. Again, this voltage was held constant until the voltage decayed to one-tenth of the initial charge current, 0.05 mA. The reversible fraction is the ratio of the first discharge capacity to the first charge capacity.

Cycling experiments were performed by repeating the same protocol until sufficient cycles were obtained to predict the cell life (or until a short circuit terminated the test). The end of life criterion was 80% of the capacity of the second cycle of the cycle test.

RESULTS AND DISCUSSION

Synthesis and Electrochemical Properties

The aqueous synthesis of nanocrystalline $M_xV_2O_5A_y \cdot nH_2O$ is easily and rapidly performed in less than 1 h by precipitation from acidified vanadate solutions. M is the cation from the starting vanadate salt, A is the anion from the mineral acid, n is ~ 0.5–1.5, and x and y are less than 0.2 and typically around 0.1. The products are red-brown in color, showing vanadium is in the $+5$ oxidation state. Although the products contain about the same amount of vanadium, the discharge capacity does depend upon the cation of the vanadium salt used in the synthesis. The highest capacities were observed when the $M_xV_2O_5A_y \cdot nH_2O$ was produced from NH_4VO_3, $LiVO_3$, or MgV_2O_6. Reversibilities were usually $>98\%$ for the first two discharge–charge cycles. Table 1 summarizes some synthesis parameters and electrochemical information for products involving $M = NH_4$, Li, and Mg and shows lithium capacities as high as ~ 380 (mA h)/g.

A typical X-ray powder diffraction pattern for $M_xV_2O_5A_y \cdot nH_2O$ is shown in Fig. 1. The weak, broad diffraction peaks indicate the crystallite size to be in the range 10–200 nm. This agrees with SEM and TEM images showing bent and curved plate crystals that are 30- to 40-nm thick (see below). From XPD data (Fig. 1), the structure of $M_xV_2O_5A_y \cdot nH_2O$ is believed to contain stacked vanadium-oxide double layers. Neighboring double layers are separated by water and by cations and anions involved in the synthesis. The proposed structure is similar to that of σ-$Zn_{0.25}V_2O_5 \cdot H_2O$ (7) and $[N(CH_3)_4]_z Mn_yV_2O_5 \cdot nH_2O$ (8), both containing some reduced vanadium. On discharge to 2 V, the capacity of the latter compound is 220 (mA h)/g compared to 280 (mA h)/g (at C/8) for $(NH_4)_{0.12}V_2O_5(SO_4)_{0.06} \cdot 0.4H_2O$.

The highest product yields of $M_xV_2O_5A_y \cdot nH_2O$, up to 97%, are achieved at H/V ratios of about 1:1 to 3:1. The compositions made in this H/V range also exhibit the highest lithium discharge capacities. Figure 2 shows the lithium discharge capacity vs H/V ratio for products having $M = NH_4$, Li, and Mg. For example, the reversible lithium capacity of an electrode made from NH_4VO_3 and H_2SO_4 at $H/V = 2$ is ~ 370 (mA h)/g (C/80 rate) (see Fig. 3), and the energy density is ~ 1000 (W h)/kg. High lithium uptake is attributed to the porous microstructure of the product. SEM images show the material to have a sponge-like, open-network microstructure composed of interconnected bent and curved plate crystals or "petals" (Fig. 4a). A TEM image of one such curved "petal" is shown in Fig. 5. In this case, the electron beam was parallel to the petal surface, and the curved (00l) planes are clearly seen.

At higher H/V levels, the yields and lithium capacities are lowered. The decrease in capacity is attributed to the formation of denser particles. This is seen in Fig. 4b for a sample made from NH_4VO_3 and H_2SO_4 at $H/V = 4$.

In the same H/V ratio range, the Na, K, and Rb vanadate solutions gave products with lower Li capacities (no higher than 300 (mA h)/g). For Na, there was a rapid drop to the 1.5-V cutoff with Li intercalation, giving a capacity of only about 260 (mA h)/g and large polarization. For K, the voltage dropped quickly in the region of 2.5 to 1.5 V, so the capacity was only about 300 (mA h)/g. The reasons for these performance differences are not known. One would have expected the K^+ to be similar to the NH_4^+ on the basis of cation charge and size if the residual cations simply occupied the interlayer regions of the $M_xV_2O_5A_y \cdot nH_2O$ product. Tetra-alkyl ammonium cations gave products that were intermediate in Li capacity (315–360 (mA h)/g).

Modifications of the synthesis method, such as the chemical doping of silver or other metals, or precipitation of $M_xV_2O_5A_y \cdot nH_2O$ in the presence of other solid materials, may further improve the final physical and electronic properties. For example, a preparation that used silver nitrate as one of the reactants gave a product with an initial discharge capacity of 390 (mA h)/g.

$M_xV_2O_5A_y \cdot nH_2O$ Composite with Carbon

In one particular modification of the synthesis, carbon black (MMM Super P) was slurried into the vanadium salt

TABLE 1
Synthesis and Electrochemical Data on $M_xV_2O_5A_y\cdot nH_2O$ (See Text for Details)

H^+/V ratio	Li discharge capacity ((mA h)/g)	Starting MVO_3	Acid used	Yield (%)	H_2O (mL)	Temp (B/°C)	Time (min)	Electrode thickness (μm)
0.7	315	$LiVO_3$, 18.2 g	HNO_3	42	450	B	5	115
0.75	264	V_2O_5, 15.6 g + $LiOH\cdot H_2O$, 7.2 g	H_2SO_4	65	900	B	35	110
1	355	$LiVO_3$, 18.2 g	H_2SO_4	97	900	B	15	115
1.1	378	V_2O_5, 50 g + $LiOH\cdot H_2O$, 23.1 g	HCl	—	350	80°C	15	90
1.4	367	NH_4VO_3, 20.1 g	HNO_3	88	450	B	5	125
1.4	340	$LiVO_3$, 18.2 g	HNO_3	89	450	B	10	110
1.4	370	NH_4VO_3, 20.1 g	HNO_3	91	900	B	20	130
1.5	383	NH_4VO_3, 8.2 g	HNO_3	—	150	B	2	120
2	365	MgV_2O_6, 18.3 g	H_2SO_4	96	900	B	15	125
2	370	NH_4VO_3, 20.1 g	H_2SO_4	92	900	B	20	130
2	374	NH_4VO_3, 20.1 g	H_2SO_4	89	900	B	60	125
2.8	350	NH_4VO_3, 20.1 g	HNO_3	73	900	B	20	115
4	325	NH_4VO_3, 20.1 g	H_2SO_4	76	900	B	20	115
4	321	$LiVO_3$, 18.2 g	H_2SO_4	62	900	B	20	100
6	272	NH_4VO_3, 20.1 g	H_2SO_4	55	900	B	20	105

solution prior to the addition of the acid. A finely dispersed powder of carbon black coated with $M_xV_2O_5A_y\cdot nH_2O$ was obtained. The amount of carbon black in the product was ~8% by weight. SEM showed the microstructure to be similar to that of the carbon-free sample (Fig. 4a). The coated-carbon product exhibits the high discharge capacity of the carbon-free material but with lower polarization evident in the 1.5- to 2.5-V range (Fig. 6). This region of voltage vs capacity corresponds to the reduction of V^{4+} to V^{3+} and, very likely, formation of an insulating phase. The lower polarization of the coated-carbon product is due to improved electronic conductivity at the lower voltage.

Interestingly, the lithium capacity of this coated-carbon material is maintained even when the rate is doubled from C/8 to C/4. For example, the lithium capacity for the carbon composite was ~325 (mA h)/g at C/8 and C/4, even though the polarization was greater at the higher rate. In comparison, the lithium capacity for the carbon-free material is lowered from 340 (mA h)/g at C/8 to 275 (mA h)/g at C/4. This rate enhancement is not attainable by simple physical mixing of carbon black with pre-made $M_xV_2O_5A_y\cdot nH_2O$.

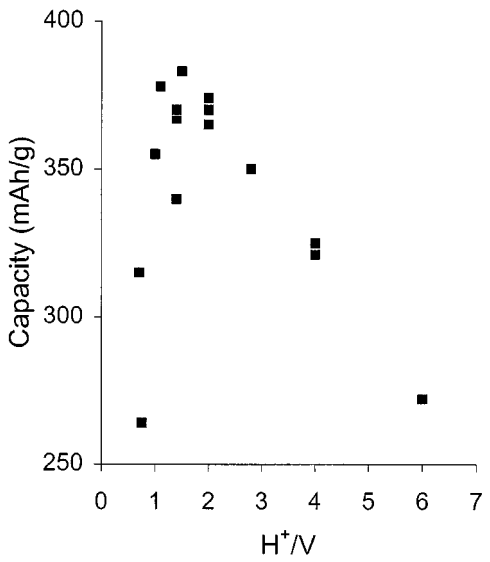

FIG. 2. Lithium discharge capacity vs H/V ratio for products having $M = NH_4$, Li, and Mg.

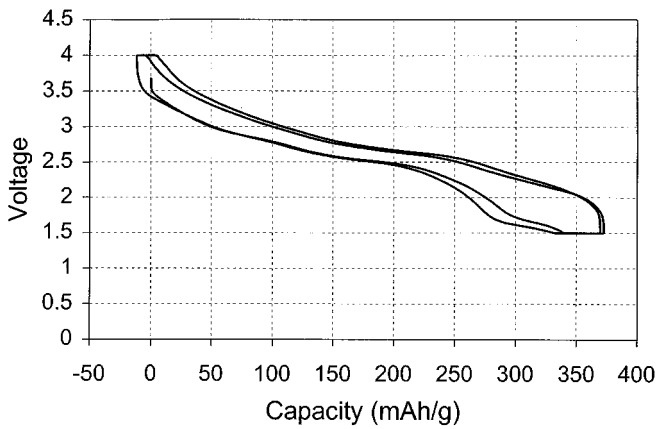

FIG. 3. Two discharge–charge cycles for $M_xV_2O_5A_y\cdot nH_2O$ showing lithium capacity of 370 (mA h)/g between 4 and 1.5 V. The constant current section of the curve is the electrochemical behavior at ~C/8 (340 (mA h)/g).

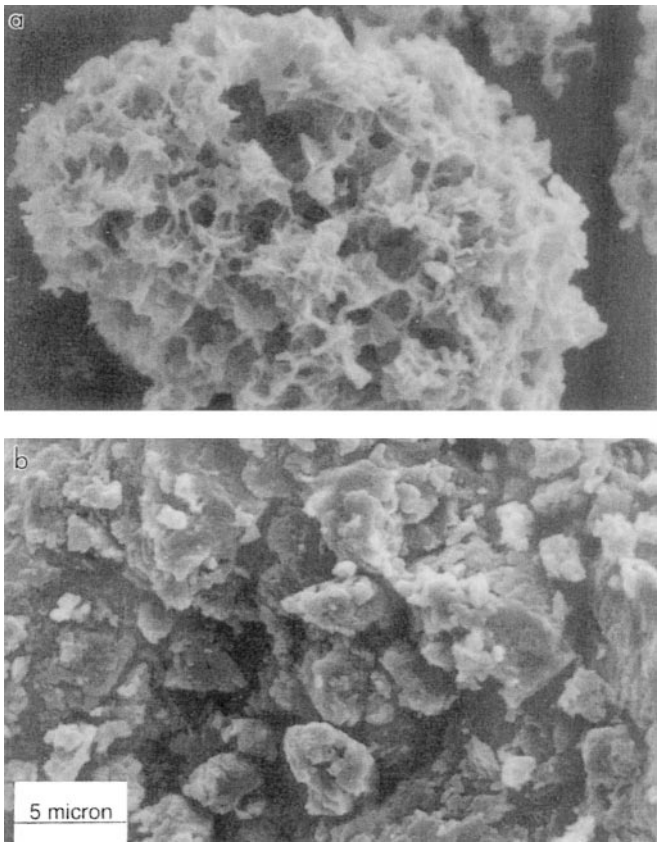

FIG. 4. (a) SEM image of $M_xV_2O_5A_y \cdot nH_2O$ made at H/V = 2 showing porous particles composed of nanocrystals. (b) SEM image of $M_xV_2O_5A_y \cdot nH_2O$ made at H/V = 4 showing dense, compacted microstructure.

Rate Test

A rate test of this $M_xV_2O_5A_y \cdot nH_2O$ coated-on-carbon cathode was conducted at room temperature by varying the discharge current from 6.4 mA (1.6C rate) to 0.05 mA (C/80 rate). See Fig. 7. Each successive discharge current increment was one-half the previous value. Each charge was run at 0.5 mA. The material performed very well, with lithium capacities of 255, 296, and 330 (mA h)/g at 1.6C, C/2, and C/80, respectively. At the slower discharge rates, additional capacity is observed on charging (see figure). This gives an apparent lithium capacity of 365 (mA h)/g. The origin of this "extra" charge is discussed below.

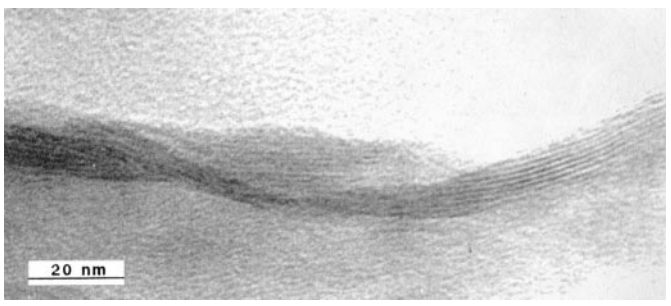

FIG. 5. TEM image of a curved plate crystal or "petal" of $M_xV_2O_5A_y \cdot nH_2O$ made from NH_4VO_3 and H_2SO_4 at H/V = 2 (see text). The curved (00l) planes are clearly seen.

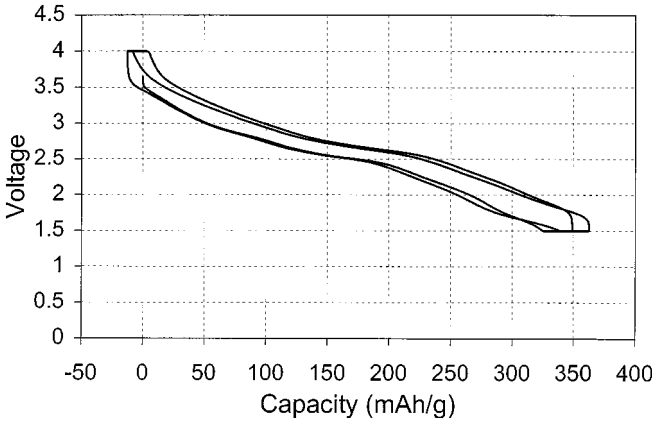

FIG. 6. Two discharge–charge cycles for $M_xV_2O_5A_y \cdot nH_2O$ coated on carbon black showing lithium capacity of 350 (mA h)/g between 4 and 1.5 V and lower polarization at lower voltage, relative to carbon-free material. The constant current section of the curve is the electrochemical behavior at ~C/8 (325 (mA h)/g).

Li-Ion Cell

Lithium metal cells are undesirable because of their reactivity and tendency to form short-circuiting dendrites when charged and discharged. Lithium alloy research is still relatively new and no good commercially viable materials are available. Pre-lithiated graphite would be a more attractive anode material because the starting compounds, Li and graphite, are cheap and sold commercially. Also, graphite is currently used in lithium-ion batteries. Here, we

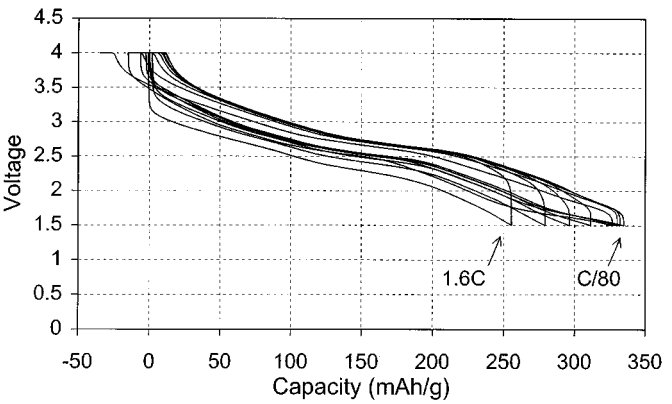

FIG. 7. Lithium capacity of $M_xV_2O_5A_y \cdot nH_2O$ coated on carbon black (4–1.5 V) as a function of discharge rate from 1.6C to C/80.

demonstrate that pre-lithiated graphite can be used as an anode with $M_xV_2O_5A_y\cdot nH_2O$/carbon cathodes.

The same $M_xV_2O_5A_y\cdot nH_2O$ coated-on-carbon film was tested as a cathode in a Li-ion electrochemical cell. The anode consisted of lithiated graphite that was formed in the coin cell by reacting at room temperature thin disks of Li metal and graphite. Graphite powder MCMB25-28 (Osaka Gas Co., Japan) was combined with Super P carbon black and EPDM rubber in cyclohexane. The graphite paste was spread onto a sheet of Teflon FEP and drawn down to form a film using a doctor blade having a 40-mil gap. The dried film consisted of 93% by weight graphite, 4% by weight binder, and 3% by weight carbon black. The film was hot-pressed under 20 psi at 110°C to form a densified electrode sheet with a thickness of about 295 μm.

In a glove box, the cathode and separator pieces were stacked along with two graphite disks and one Li disk, the Li disk having a thickness of about 100 μm, into coin-cell pans with electrolyte solution ($LiPF_6$ in EC/DMC) and sealed under pressure as described above. The coin cells were allowed to stand for 90 h before testing. This allowed sufficient time for the lithium metal to react completely with the graphite. In graphite intercalation, LiC_6 is the composition of the most Li-rich phase. The quantities of graphite and Li metal used in our experiments gave a composition of $\sim LiC_{10}$ to ensure that no Li metal would remain in the coin cell prior to testing. The electrodes were not electrochemically balanced in the coin cell, and an excess of lithiated graphite was present, relative to the quantity of Li required for complete discharge. The coin cells were tested according to the standard method employed above except that the voltage range was adjusted from 1.5–4.0 V to 1.4–3.9 V because the voltage of the lithium-graphite anode was observed to be about 0.09 V relative to Li metal. Under the unoptimized coin-cell assembly just described, 92% of the initial discharge capacity obtained in the Li-metal cell was observed for the Li-ion cell.

Cycle Life

Cycle life (the number of discharge and charge cycles that it takes to get to 80% of the original capacity) is less than 100 for the high-capacity materials made at H/V $\sim$2. Under high-acid synthesis conditions, e.g., H/V $\sim$4, the cycle life can reach 250 cycles in a narrower voltage range (310 (mA h)/g, 3.75–1.75 V). However, under these high-acid conditions the lithium capacity, product yield, and reversibility are no longer maximized. So there are separate optimum synthesis conditions for Li capacity and for cycle life.

The high-acid effect of increasing cycle life is not clearly understood. There is evidence to suggest an oxidative-degradation reaction occurs between pentavalent vanadium and the solvent and/or binder. This is seen as "extra" capacity at the end of the charge cycle when the electrodes are charged to 4.0 V at slow rates ($\sim$C/80) (see Figs. 3 and 6). Such a redox reaction is expected to be dependent on the surface area of the active material. Higher surface area $M_xV_2O_5A_y\cdot nH_2O$ is obtained at lower H/V ratios. For example, the surface areas for products made using NH_4VO_3 and H_2SO_4 at H/V = 2 and H/V = 4 are 6.5 and 1.4 m^2/g, respectively. This difference in surface area is also reflected in the SEM images (Fig. 4). The best cycle life (255 cycles) came from $M_xV_2O_5A_y\cdot nH_2O$ having a surface area of 0.15 m^2/g. The "extra" charge capacity is lowered or not seen at cycling rates faster than $\sim$C/10. This is because the electrode does not stay in the 4-V region for a long time. Lowering the maximum voltage to 3.75 V also decreases the rate of these oxidation–reduction side reactions.

Other redox reactions affecting cycle life may be the oxidation of the residual water in the $M_xV_2O_5A_y\cdot nH_2O$ or oxidation of ammonium when using NH_4VO_3 in the synthesis. In the process described earlier for making our coin cells, we find $n \sim 0.1$–0.4 (Karl–Fischer titrations) and $x \sim 0.1$ in $M_xV_2O_5A_y\cdot nH_2O$ ($M = NH_4^+$).

In addition to oxidation–degradation reactions, the volumetric changes that occur in the crystals and particles, by the removal of water, and by the insertion and removal of lithium, may lead to stresses that cause the electrode to disintegrate. From TGA and XPD data, we see the interlayer d spacing of $V_2O_5\cdot nH_2O$ decrease significantly when the water is removed. For example, material made from NH_4VO_3 and H_2SO_4 at H/V = 2 shows a change in this d spacing from 11.2 to 10.0 Å as n goes from $\sim$0.8 to 0. For products made from $LiVO_3$, the change is even larger, 12.1 to 9 Å. At least another 1-Å decrease, e.g., 10.0 to 9.0 Å, occurs when lithium is inserted between the layers as seen by XPD of discharged coin-cell electrodes.

We have focused on keeping the lithium capacity high while trying to increase cycle life. Therefore, we have used wide voltage ranges (4–1.5 V and 3.75–1.75 V). The material made at H/V $\sim$1–2 may cycle well in a narrower voltage range while delivering a reduced capacity (i.e., there may be a capacity vs cycle life trade-off at any given H/V ratio). Our research is now directed toward understanding and controlling the parameters that influence cycle life.

ACKNOWLEDGMENT

We thank Marc Doyle and Mark Roelofs for many helpful battery discussions, Rick Maynard for surface area measurements, Catherine Foris, John Longacre, and Dennis Redmond for X-ray powder diffraction data, and Richard Harlow for powder X-ray synchrotron diffraction data.

REFERENCES

1. J. Livage, *Chem. Mater.* **3,** 578 (1991).
2. B. B. Owens, S. Passerini, and W. H. Smyrl, *Electrochim. Acta* **45,** 215 (1999).

3. M. Giorgetti, S. Passerini, W. H. Smyrl, S. Mukerjee, X. Q. Yang, and J. McBreen, *J. Electrochem. Soc.* **146,** 2387 (1999).
4. F. A. Cotton and G. Wilkinson, "Advanced Inorganic Chemistry," 4th ed., p. 711. Wiley, New York, 1980.
5. N. Kishimoto and E. Matsunami, European Patent, EP 747123, 1996.
6. F. Théobald, *Bull. Soc. Chim. France* No. 7–8, 1607 (1975).
7. Y. Oka, O. Tamada, T. Yao, and N. Yamamoto, *J. Solid State Chem.* **126,** 65 (1996).
8. F. Zhang and M. S. Whittingham, *Electrochem. Commun.* **2,** 69 (2000).